Spatial Spectrum Sensing-Based D2D Communications in User-Centric Deployed HetNets

Bodong Shang*, Lingjia Liu*, Hao Chen †, Jianzhong (Charlie) Zhang †,
Scott Pudlewski ‡, Elizabeth Serena Bentley ‡, and Jonathan Ashdown ‡
*The Bradley Department of Electrical and Computer Engineering, Virginia Tech, Blacksburg VA, 24061, USA
†Samsung Research America, Richardson, TX, 75082, USA
‡Information Directorate, Air Force Research Laboratory, Rome, NY 13441, USA

***Abstract*—This paper develops a novel framework for the modeling and analysis of spatial spectrum sensing (SSS) for device-to-device (D2D) communications in uplink two-tier user-centric deployed heterogeneous networks (HetNets), where small cell base stations (SBSs) are deployed in the places with high user density termed hotspots introduced by 3GPP. We study the average transmit power of uplink users, the probability of spatial false alarm and the probability of spatial miss detection of a typical D2D transmitter (D2D-Tx) during SSS. Based on the results, we further characterize the coverage probability of a typical D2D user and the area spectral efficiency (ASE) of D2D networks. Simulation results verify our analysis and demonstrate the advantages of SSS-based D2D communications in future wireless networks.**

***Index Terms*—D2D communications, spatial spectrum sensing, heterogeneous cellular networks, Poisson cluster process.**

I. Introduction

Implementing device-to-device (D2D) communications in cellular networks can improve the overall spectrum utilization efficiency and alleviate the traffic burden at base stations (BSs) by the physical proximity of communicating devices and the reduced data transmissions through BSs [1]. However, there are still some technical issues for integrating D2D communications into cellular networks, such as cross mode interference management, willingness of content sharing [2], limited energy constraint of D2D devices [3] and spectrum access [4], etc. In this paper, we focus on the spectrum access as well as interference management of D2D communications, where D2D transmitters (D2D-Txs) reuse the licensed uplink cellular spectrum based on spatial spectrum sensing (SSS).

In cellular networks, the coverage-driven deployment of macrocells is gradually becoming less able to satisfy the upsurge growth of cellular data traffic. To reuse the spectral resources more aggressively, a user-centric capacity-driven deployment of small cells has attracted great attention, where the low power types of BSs are deployed in the areas of high user density (termed hotspots) [5]. Along with the ubiquitous coverage blanket of uniformly deployed macro BSs (MBSs), the small cell BSs (SBSs) exhibit flexibility in the deployment and generate correlations between hotspot users and SBSs locations. The resulting cellular networks consisting of different tiers is referred to as heterogeneous networks (HetNets). Such user-centric deployment of SBSs is more realistic and generalizes the state-of-the-art approaches in 3GPP simulation scenarios.

However, how to reuse the licensed spectrum efficiently for D2D communications in HetNets while reducing the cross mode interference with cellular communications is of significance in the future wireless network design [6]. In [7], the approach of providing guard zones (protection regions) around cellular BSs was introduced. However, this approach needs the geometry information of D2D-Txs and MBSs. In [8], [9], a QoS-aware approach for D2D spectrum access was presented. However, the approach considers the uniformly distributed macrocells network. The performance of D2D spectrum access in more realistic network scenarios such as correlated HetNets still remains unknown.

In this paper, we model and analyze the SSS-based D2D communications in two-tier user-centric deployed HetNets, where SBSs and hotspot users are clustered around each cluster center independently overlaid on a uniformly distributed MBSs. We summarize the contributions as follows:

- We first obtain the average uplink transmit power of cellular users. For the performance of SSS, we characterize the probability of spatial false alarm and the probability of spatial miss detection of SSS-based D2D communications in two-tier user-centric deployed HetNets.
- Based on the results, we derive the coverage probability of D2D networks. In addition, the area spectral efficiency (ASE) of D2D networks is also quantified. To the best of our knowledge, this is the first work which extends the analysis of SSS to HetNets. Simulation and numerical results are presented to demonstrate the performance of SSS-based D2D networks and verify our analysis.

The remainder of this paper is organized as follows. In Section II, system model is presented. Section III formulates the probabilities of spatial false alarm and miss detection of SSS-based D2D communications. Section IV shows the coverage probability of a typical D2D user and ASE of D2D networks. Simulation and numerical results are shown in Section V. Finally, conclusions are drawn in Section VI.

The work of B. Shang and L. Liu are supported in part by U.S. National Science Foundation (NSF) under grants ECCS-1802710, ECCS-1811497, and CNS-1811720. Any opinions, findings and conclusions or recommendations expressed in this material are those of the authors and do not necessarily reflect the views of AFRL. Approved for public release; distribution unlimited: 88ABW-2019-3113).

978-1-7281-0962-6/19/$31.00 ©2019 IEEE

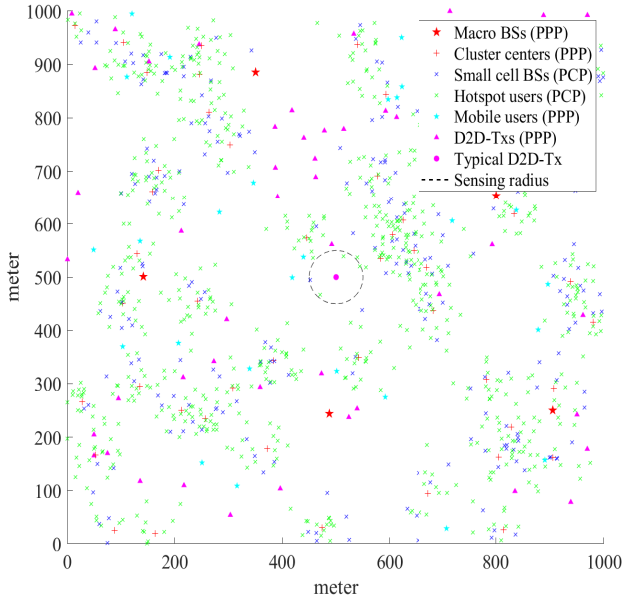

Fig 1: System model of SSS-based D2D communications in user-centric deployed HetNet.

II. System Model and Spatial Spectrum Sensing

A. System Model

1) Network layout: We consider that D2D communications reuse cellular uplink channel. The network architecture is shown in Fig. 1. The locations of MBS are modeled as a homogeneous Poisson point process (PPP) with the density of λ_m and are denoted as the set of $\Phi_{\mathrm{m}} = \left\{b_j^m\right\}$. The locations of cluster centers being the parent point process for clusters are modeled as a homogeneous PPP with the density of λ_p denoted by $\Phi_{\mathrm{p}} = \{x_j\}$. To capture the coupling between SBSs and hotspot users, we model the locations of SBSs and hotspot users as two Poisson cluster processes (PCPs) with the same cluster centers Φ_{p}. The set of SBSs is denoted by $\Phi_{\mathrm{s}} = \{\Phi_{\mathrm{s}}^{x_1}, \Phi_{\mathrm{s}}^{x_2}, ...\}$, where $\Phi_{\mathrm{s}}^{x_j} = \left\{b_{i,j}^s\right\}$ represents the set of SBSs attached to cluster center x_j. The set of hotspot users is denoted by $\Phi_{\mathrm{u}}^H = \{\Phi_{\mathrm{u}}^{x_1}, \Phi_{\mathrm{u}}^{x_2}, ...\}$, where $\Phi_{\mathrm{u}}^{x_j} = \{u_{l,j}\}$ represents the set of hotspot users attached to cluster center x_j. The average number of SBSs and hotspot users per cluster are n_b and n_u, respectively. In this paper, we focus on the modified Thomas cluster process (TCP) [10] with independent Gaussian distribution:

$$\begin{aligned} f_{b_{i,j}^s}\left(b_{i,j}^s\right) &= \frac{1}{2\pi {\sigma_s}^2} \exp\left(-\frac{\left\|b_{i,j}^s\right\|^2}{2{\sigma_s}^2}\right), b_{i,j} \in \mathbb{R}^2 \\ f_{u_{l,j}}\left(u_{l,j}\right) &= \frac{1}{2\pi {\sigma_u}^2} \exp\left(-\frac{\left\|u_{l,j}\right\|^2}{2{\sigma_u}^2}\right), u_{l,j} \in \mathbb{R}^2, \end{aligned} \tag{1}$$

where $f_{b_{i,j}^s}\left(b_{i,j}^s\right)$ and $f_{u_{l,j}}\left(u_{l,j}\right)$ are the probability density function (PDF) of each SBS and hotspot user conditioned on x_j, respectively. $\sigma_s\,(\sigma_u)$ denotes the scattering variance of the locations of SBSs (hotspot users) around each cluster center. Mobile users and D2D-Txs are modeled as two independent homogeneous PPPs, i.e., $\Phi_{\mathrm{u}}^M = \{u_l\}$ and $\Phi_{\mathrm{d}} = \{d_k\}$, with the density of λ_u and λ_d, respectively. Each D2D-Tx has the transmit power P_d and the sensing radius $\mathcal{R}_s$. The sensing region $\mathcal{A}_{d_k}$ of a typical D2D-Tx d_k is given by $\mathcal{A}_{d_k} = \mathcal{B}\left(d_k, \mathcal{R}_s\right)$, where $\mathcal{B}\left(d_k, \mathcal{R}_s\right) = \left\{x \in \mathbb{R}^2 \middle| \left\|d_k - x\right\| \leqslant \mathcal{R}_s\right\}$.

2) User association and propagation model: We assume that each hotspot user can connect to the nearest SBS within its attached cluster or the nearest MBS. The setup is inspired by the situations where SBSs are enterprise-owned BSs serving authorized users. Each mobile user connects to the nearest MBS in uplinks. We consider the semi-static power control mechanism for uplink transmissions. The transmit power of a cellular user is $P_u = P_0 {X_u}^{\eta\alpha}, 0 \leqslant \eta \leqslant 1$ [11], where P_0 is the basic transmit power of a cellular user before applying power control, X_u is the serving distance, η is the power control fraction, and α is the path-loss exponent.

The signal-to-interference-plus-noise ratio (SINR) of a typical D2D user u_k^d associated with d_k is given by

$$SINR\left(u_k^d\right) = \frac{P_d h_{d_k u_k^d} \left\|d_k - u_k^d\right\|^{-\alpha}}{I_{u_k^d}^C + I_{u_k^d}^D + {\sigma_n}^2}, \tag{2}$$

where $h_{d_k u_k^d} \sim \exp\left(1\right)$ is the channel power gain, $\left\|d_k - u_k^d\right\|$ indicates the serving distance between d_k and u_k^d, $I_{u_k^d}^C = I_{u_k^d}^{C,m} + I_{u_k^d}^{C,s}$ denotes the interference from cellular network consisting of the interference from MBSs $I_{u_k^d}^{C,m} = \sum_{u_l^m \in \Phi_{\mathrm{um}}} P_{u_l^m} h_{u_l^m d_k} \left\|u_l^m - d_k\right\|^{-\alpha}$ and the interference from SBSs $I_{u_k^d}^{C,s} = \sum_{x_j \in \Phi_{\mathrm{p}}} \sum_{u_{l,j}^s \in \Phi_{\mathrm{us}}^{x_j}} P_{u_{l,j}^s} h_{u_{l,j}^s d_k} \left\|u_{l,j}^s - d_k\right\|^{-\alpha}$, Φ_{um} is the set of scheduled users connected to MBSs and $\Phi_{\mathrm{us}} = \{\Phi_{\mathrm{us}}^{x_1}, \Phi_{\mathrm{us}}^{x_2}, ...\}$ is the set of scheduled users connected to SBSs, $I_{u_k^d}^D$ represents the interference from active D2D-Txs and ${\sigma_n}^2$ is the variance of noise power.

B. Spatial Spectrum Sensing

Let $\mathcal{H}^0$ be the event that there is no active cellular user in the sensing region $\mathcal{A}_{d_k}$, and $\mathcal{H}^1$ be the event that there is at least one active cellular user in $\mathcal{A}_{d_k}$. We assume that all D2D-Txs can perform SSS in a duration τ seconds at the beginning of each time-slot T simultaneously and transmit data in the remaining $T - \tau$ seconds. The received signals during SSS at d_k under $\mathcal{H}^0$ and $\mathcal{H}^1$ are given in (3) and (4) on the top of next page, respectively, where n is index of samples, $s_{u_l^m}[n]$ and $s_{u_{l,j}^s}[n]$ are the n^{th} samples from scheduled cellular users u_l^m and $u_{l,j}^s$ associated with MBS and SBS, respectively, $\Phi_{\mathrm{u}} = \{\Phi_{\mathrm{um}} \cup \Phi_{\mathrm{us}}\}$, $P_{u_l^m}$ and $P_{u_{l,j}^s}$ indicate the transmit powers of u_l^m and $u_{l,j}^s$, respectively, and noise $n_0[n]$ is i.i.d. circularly symmetric complex Gaussian with mean 0 and variance ${\sigma_n}^2$. The distribution of the test statistics $\Gamma|\, I^\chi = \frac{1}{N}\sum_{n=0}^{N-1} |y[n]|^2$ approaches to Gaussian distribution according to central limit theorem, i.e., $\Gamma|\, I^\chi \sim \mathcal{N}\left(I^\chi + {\sigma_n}^2, \frac{\left(I^\chi + {\sigma_n}^2\right)^2}{N}\right), \chi = 0, 1$, where

$$\begin{aligned} I^0 = &\sum_{u_l^m \in \Phi_{\mathrm{um}}, u_l^m \notin \mathcal{A}_{d_k}} P_{u_l^m} h_{u_l^m d_k} \left\|u_l^m - d_k\right\|^{-\alpha} \\ &+ \sum_{x_j \in \Phi_{\mathrm{p}}} \sum_{u_{l,j}^s \in \Phi_{\mathrm{us}}^{x_j}, u_{l,j}^s \notin \mathcal{A}_{d_k}} P_{u_{l,j}^s} h_{u_{l,j}^s d_k} \left\|u_{l,j}^s - d_k\right\|^{-\alpha}, \end{aligned} \tag{5}$$

$$\mathcal{H}^0 : y[n] = \sum_{\substack{u_l^m \in \Phi_{\text{um}} \\ u_l^m \notin \mathcal{A}_{d_k}}} \sqrt{\frac{P_{u_l^m} h_{u_l^m d_k}}{\|u_l^m - d_k\|^\alpha}} s_{u_l^m}[n] + \sum_{x_j \in \Phi_{\text{p}}} \sum_{\substack{u_{l,j}^s \in \Phi_{\text{us}}^{x_j} \\ u_{l,j}^s \notin \mathcal{A}_{d_k}}} \sqrt{\frac{P_{u_{l,j}^s} h_{u_{l,j}^s d_k}}{\left\|u_{l,j}^s - d_k\right\|^\alpha}} s_{u_{l,j}^s}[n] + n_0[n], \tag{3}$$

$$\mathcal{H}^1 : y[n] = \sum_{\substack{u_l^m \in \Phi_{\text{um}} \\ \Phi_{\text{u}} \cap \mathcal{A}_{d_k} \neq \emptyset}} \sqrt{\frac{P_{u_l^m} h_{u_l^m d_k}}{\|u_l^m - d_k\|^\alpha}} s_{u_l^m}[n] + \sum_{x_j \in \Phi_{\text{p}}} \sum_{\substack{u_{l,j}^s \in \Phi_{\text{us}}^{x_j} \\ \Phi_{\text{u}} \cap \mathcal{A}_{d_k} \neq \emptyset}} \sqrt{\frac{P_{u_{l,j}^s} h_{u_{l,j}^s d_k}}{\left\|u_{l,j}^s - d_k\right\|^\alpha}} s_{u_{l,j}^s}[n] + n_0[n]. \tag{4}$$

$$I^1 = \sum_{u_l^m \in \Phi_{\text{um}}, \Phi_{\text{u}} \cap \mathcal{A}_{d_k} \neq \emptyset} P_{u_l^m} h_{u_l^m d_k} \|u_l^m - d_k\|^{-\alpha} + \sum_{x_j \in \Phi_{\text{p}}} \sum_{u_{l,j}^s \in \Phi_{\text{us}}^{x_j}, \Phi_{\text{u}} \cap \mathcal{A}_{d_k} \neq \emptyset} P_{u_{l,j}^s} h_{u_{l,j}^s d_k} \left\|u_{l,j}^s - d_k\right\|^{-\alpha}. \tag{6}$$

Note that I^0 and I^1 are random variables depending on the network topology and channel fading. The probability of spatial false alarm and the probability of spatial miss detection are expressed as

$$P_{fa} = \mathbb{E}_{I^0}\left\{\mathbb{P}\left(\Gamma > \varepsilon \middle| \mathcal{H}^0, I^0\right)\right\}, \tag{7}$$

$$P_{md} = \mathbb{E}_{I^1}\left\{\mathbb{P}\left(\Gamma < \varepsilon \middle| \mathcal{H}^1, I^1\right)\right\}, \tag{8}$$

where ε is the energy detection threshold.

If the test statistic Γ at a D2D-Tx is greater than ε, the D2D-Tx will transmit with probability β_1, otherwise, it will transmit with probability β_0, where $\beta_0 > \beta_1$. Therefore, under event $\mathcal{H}^0$, a D2D-Tx will access the channel with probability $P_d^0 = P_{fa}\beta_1 + (1 - P_{fa})\beta_0$. Under event $\mathcal{H}^1$, a D2D-Tx will access the channel with probability $P_d^1 = (1 - P_{md})\beta_1 + P_{md}\beta_0$.

III. Preliminary results for SSS-based D2D

In this section, we provide intermediate technical results for our system-level performance analysis, which will be used to determine the coverage probability and ASE of D2D networks.

A. Average Transmit Power of Uplink Users

Lemma 1. *The average uplink transmit powers of cellular users associated with MBSs $\mathbb{E}\{P_{um}\}$ and SBSs $\mathbb{E}\{P_{us}\}$ are*

$$\mathbb{E}\{P_{um}\} = \frac{\lambda_u}{\lambda_u^m}\mathbb{E}\left\{P_{um}^M\right\} + \frac{n_u \lambda_p \mathbb{E}_\zeta\left\{\mathcal{A}_{u_{l,j}}^m\right\}}{\lambda_u^m}\mathbb{E}\left\{P_{um}^H\right\}, \tag{9}$$

$$\mathbb{E}\{P_{us}\} = P_0 \int_0^\infty \int_0^\infty f_\zeta(\zeta) f_{R_{u_{l,j}}^s}(r|\zeta) r^{\eta\alpha} dr d\zeta, \tag{10}$$

where $\lambda_u^m = \lambda_u + n_u\lambda_p\mathbb{E}_\zeta\left\{\mathcal{A}_{u_{l,j}}^m\right\}$ is the density of users associated with MBSs, $\mathbb{E}\left\{P_{um}^M\right\} = P_0\int_0^\infty f_{B_m}(r) r^{\eta\alpha} dr$ is the average transmit power of mobile users, $\mathbb{E}\left\{P_{um}^H\right\} = P_0\int_0^\infty\int_0^\infty f_\zeta(\zeta) f_{R_{u_{l,j}}^m}(r|\zeta) r^{\eta\alpha} dr d\zeta$ is the average transmit power of a typical hotspot user connected to a MBS, $\mathbb{E}_\zeta\left\{\mathcal{A}_{u_{l,j}}^m\right\} = \int_0^\infty f_\zeta(\zeta)\mathcal{A}_{u_{l,j}}^m(\zeta)d\zeta$ and $f_\zeta(\zeta) = \frac{\zeta}{{\sigma_u}^2}\exp\left(-\frac{\zeta^2}{2{\sigma_u}^2}\right), \zeta \geqslant 0$.

Proof: The conditional probability that a hotspot user $u_{l,j}$ connects to a macro BS is given by

$$\mathcal{A}_{u_{l,j}}^m \middle| \zeta_{l,j} = \mathbb{P}\left\{u_{l,j} \in \widehat{\Phi}_{\text{um}} \middle| \zeta_{l,j} = \|u_{l,j} - x_j\|\right\} = 1 - \int_0^\infty f_{B_m}(r) F_{B_s}(r|\zeta_{l,j}) dr, \tag{11}$$

where $\widehat{\Phi}_{\text{um}}$ denotes the set of users associated with MBSs, $f_{B_m}(r) = 2\pi\lambda_m r e^{-\pi\lambda_m r^2}, r \geqslant 0$, $F_{B_s}(r|\zeta_{l,j}) = 1 - Q_1\left(\frac{\zeta_{l,j}}{\sigma_s}, \frac{r}{\sigma_s}\right)^{n_b}, r \geqslant 0$, $Q_1(a,b) = \int_b^\infty t e^{-\frac{t^2+a^2}{2}} I_0(at) dt$ is the Marcum Q-function and $I_0(\cdot)$ is the modified Bessel function of the first kind with order zero, and $\zeta_{l,j} = \|u_{l,j} - x_j\|$. We fix the number of SBSs per cluster equal to n_b to simplify the order statistic arguments with the tractability in analysis, and we will show the impact of this approximation in simulations where the number of SBSs per cluster follows a Poisson distribution with the mean value of n_b. In addition, the conditional probability that a hotspot user $u_{l,j}$ connects to a SBS is $\mathcal{A}_{u_{l,j}}^s \middle| \zeta_{l,j} = 1 - \mathcal{A}_{u_{l,j}}^m \middle| \zeta_{l,j}$.

For a typical hotspot user $u_{l,j}$ located at distance $\zeta_{l,j}$ from its cluster center, conditioned on the association with MBSs, i.e., $\mathcal{A}_{u_{l,j}}^m \middle| \zeta_{l,j}$, the conditional complementary cumulative distribution function (CCDF) of its serving distance $R_{u_{l,j}}^m$ is:

$$\mathbb{P}\left\{R_{u_{l,j}}^m > r_{u_{l,j}}^m \middle| u_{l,j} \in \widehat{\Phi}_{\text{um}}, \zeta_{l,j}\right\} = \frac{\int_{r_{u_{l,j}}^m}^\infty \mathbb{P}\{R_{B_s} > r_{B_m} | \zeta_{l,j}\} f_{B_m}(r_{B_m}) dr_{B_m}}{\mathcal{A}_{u_{l,j}}^m \middle| \zeta_{l,j}}, \tag{12}$$

and the PDF of serving distance $R_{u_{l,j}}^m$ of hotspot user $u_{l,j}$ associated with a MBS is

$$f_{R_{u_{l,j}}^m}\left(r_{u_{l,j}}^m \middle| \zeta_{l,j}\right) = \frac{\partial \mathbb{P}\left\{R_{u_{l,j}}^m \leqslant r_{u_{l,j}}^m \middle| u_{l,j} \in \widehat{\Phi}_{\text{um}}, \zeta_{l,j}\right\}}{\partial r_{u_{l,j}}^m} \tag{13}$$

Using a similar method, we can derive the PDF of the serving distance of a hotspot user $u_{l,j}$ associated with a SBS, i.e., $f_{R_{u_{l,j}}^s}\left(r_{u_{l,j}}^s \middle| \zeta_{l,j}\right)$. The results in Lemma 1 are obtained by taking an average of $R_{u_{l,j}}^m$, $R_{u_{l,j}}^s$ and $\zeta_{l,j}$. ■

B. Probability of Spatial False Alarm

Proposition 1. *The Laplace transform of I^0 is given in (14) as follows, where $f_{U_s}(r|x) = \frac{r}{{\sigma_u}^2}\exp\left(-\frac{r^2+x^2}{2{\sigma_u}^2}\right) I_0\left(\frac{rx}{{\sigma_u}^2}\right)$.*

$$\mathcal{L}_{I^0}(s) \approx \underbrace{e^{-\frac{2\pi\lambda_m \mathbb{E}\{P_{um}\} s}{(\alpha-2)\mathcal{R}_s{}^{\alpha-2}} {}_2F_1\left(1, 1-\frac{2}{\alpha}; 2-\frac{2}{\alpha}; -\frac{s\mathbb{E}\{P_{um}\}}{\mathcal{R}_s{}^\alpha}\right)}}_{\mathcal{L}_{I_m^0}(s)} \cdot \underbrace{e^{-2\pi\lambda_p \int_0^\infty \left[1 - \exp\left(-n_b \int_{\mathcal{R}_s}^\infty \frac{f_{U_s}(r|x) r^\alpha}{r^\alpha + s\mathbb{E}\{P_{us}\}} dr\right)\right] x dx}}_{\mathcal{L}_{I_s^0}(s)}. \tag{14}$$

Proof: Note that, in (5), $I^0 = I_m^0 + I_s^0$, where I_m^0 (I_m^1) represents the received power from MBSs (SBSs) at a typical

D2D-Tx under $\mathcal{H}^0$ ($\mathcal{H}^1$). The Laplace transform of I^0 can be expressed as $\mathcal{L}_{I^0}(s) = \mathcal{L}_{I_m^0}(s)\,\mathcal{L}_{I_s^0}(s)$. Using Jensen's inequality and approximating Φ_{um} into a PPP with the density of λ_m, we can obtain the result in (14). ∎

Leveraging the inverse Laplace transform, we can express the probability of spatial false alarm at a typical D2D-Tx as

$$P_{fa} = \int_0^\infty \int_0^\infty Q\left(\frac{\varepsilon - x - {\sigma_n}^2}{x + {\sigma_n}^2}\sqrt{N}\right) \frac{\mathcal{L}_{I^0}(2i\pi t)}{2\pi e^{-2i\pi x t}} dt dx, \tag{15}$$

where $Q(\cdot)$ is the Q-function. However, (15) is inefficient to calculate, since it involves multiple integrals. We then introduce an approximation for the distribution of I^0, which is tractable and accurate in analysis and verified by simulations.

Proposition 2. *An approximated PDF of I^0 is proposed as*

$$f_{I^0}(x) \approx \int_0^x f_{I_m^0}(x-y)\, f_{I_s^0}(y) dy, \tag{16}$$

where $f_{I_m^0}(\cdot)$ is the PDF of I_m^0 and $f_{I_s^0}(\cdot)$ is the PDF of I_s^0.

Proof: The results can be obtained by approximating that I_m^0 and I_s^0 are independent variables. ∎

Specifically, $f_{I_m^0}(\cdot)$ is given in [10] and $f_{I_s^0}(\cdot)$ can be approximated by an inverse Gaussian distribution as follows

$$f_{I_s^0}(x) \approx \sqrt{\frac{\lambda_s^0}{2\pi x^3}} \exp\left[\frac{-\lambda_s^0 \left(x - \mu_s^0\right)^2}{2(\mu_s^0)^2 x}\right], \tag{17}$$

where the parameters μ_s^0 and λ_s^0 can be trained by machine learning method.

Corollary 1. *The probability of spatial false alarm can be approximated as*

$$P_{fa} \approx \int_0^\infty Q\left(\frac{\varepsilon - x - {\sigma_n}^2}{x + {\sigma_n}^2}\sqrt{N}\right) f_{I^0}(x) dx, \tag{18}$$

where $f_{I^0}(x)$ is given in Proposition 2.

To balance the performance of false alarm and miss detection, we consider the well-known Neyman-Pearson criterion [12] applied at D2D-Tx, i.e., $P_{fa} = P_{fa}^*$, where P_{fa}^* is the threshold of the false alarm probability, and thus the energy detection threshold ε can be obtained numerically given P_{fa}^*.

C. Probability of Spatial Miss Detection

Under event $\mathcal{H}^1$, we consider three cases for the derivation of the probability of spatial miss detection.

1) Case 1: In the sensing region $\mathcal{A}_{d_k}$, there is at least one scheduled uplink user associated with MBS, but there is no scheduled uplink user associated with SBS.

The probability of case 1 is given by

$$\begin{aligned}\mathbb{P}\{Case\ 1\} &= \mathbb{P}\left\{\Phi_{\text{um}} \cap \mathcal{A}_{d_k} \neq \emptyset, \Phi_{\text{us}} \cap \mathcal{A}_{d_k} = \emptyset \middle|\, \mathcal{H}^1\right\} \\ &= \frac{\left(1 - \mathbb{P}\{\Phi_{\text{um}} \cap \mathcal{A}_{d_k} = \emptyset\}\right) \mathbb{P}\{\Phi_{\text{us}} \cap \mathcal{A}_{d_k} = \emptyset\}}{1 - \mathbb{P}\{\mathcal{H}^0\}},\end{aligned} \tag{19}$$

where we have $\mathbb{P}\{\Phi_{\text{um}} \cap \mathcal{A}_{d_k} = \emptyset\} = e^{-\pi\lambda_m {\mathcal{R}_s}^2}$, $\mathbb{P}\{\Phi_{\text{us}} \cap \mathcal{A}_{d_k} = \emptyset\} = e^{-\lambda_p 2\pi \int_0^\infty x\left(1 - Q_1\left(\frac{x}{\sigma_u}, \frac{\mathcal{R}_s}{\sigma_u}\right)^{n_b}\right) dx}$, and $\mathbb{P}\left\{\mathcal{H}^0\right\} = \mathbb{P}\{\Phi_{\text{um}} \cap \mathcal{A}_{d_k} = \emptyset\}\,\mathbb{P}\{\Phi_{\text{us}} \cap \mathcal{A}_{d_k} = \emptyset\}$.

Proposition 3. *the PDF of I^1 in case 1 can be obtained as follows*

$$f_{I_{C_1}^1}(x) = \int_0^x f_{I_m^1}(x-y)\, f_{I_s^0}(y) dy, \tag{20}$$

where $f_{I_m^1}(\cdot)$ denotes the aggregated interference power generated from Φ_{um} conditioned on that there is at least one user in Φ_{um} located in $\mathcal{A}_{d_k}$ [13].

2) Case 2: In $\mathcal{A}_{d_k}$, there is no scheduled uplink user associated with MBS, but there is at least one scheduled uplink user associated with SBS.

The probability of case 2 is given by

$$\mathbb{P}\{Case\ 2\} = \frac{\mathbb{P}\{\Phi_{\text{um}} \cap \mathcal{A}_{d_k} = \emptyset\}\left(1 - \mathbb{P}\{\Phi_{\text{us}} \cap \mathcal{A}_{d_k} = \emptyset\}\right)}{1 - \mathbb{P}\{\mathcal{H}^0\}}. \tag{21}$$

Proposition 4. *In case 2, the PDF of I^1 can be obtained as follows*

$$f_{I_{C_2}^1}(x) = \int_0^x f_{I_m^0}(x-y)\, f_{I_s^1}(y) dy, \tag{22}$$

where $f_{I_s^1}(\cdot)$ can be approximated by an inverse Gaussian distribution as follows

$$f_{I_s^1}(x) \approx \sqrt{\frac{\lambda_s^1}{2\pi x^3}} \exp\left[\frac{-\lambda_s^1 \left(x - \mu_s^1\right)^2}{2(\mu_s^1)^2 x}\right], \tag{23}$$

where the mean and the shape parameters μ_s^1 and λ_s^1 can be obtained by machine learning method.

3) Case 3: In $\mathcal{A}_{d_k}$, there is at least one scheduled uplink user associated with MBS, and there is at least one scheduled uplink user associated with SBS.

The probability of case 3 is given by

$$\begin{aligned}\mathbb{P}\{Case\ 3\} &= \left(1 - \mathbb{P}\{\Phi_{\text{um}} \cap \mathcal{A}_{d_k} = \emptyset\}\right) \\ &\quad \cdot \frac{\left(1 - \mathbb{P}\{\Phi_{\text{us}} \cap \mathcal{A}_{d_k} = \emptyset\}\right)}{1 - \mathbb{P}\{\mathcal{H}^0\}}.\end{aligned} \tag{24}$$

Proposition 5. *In case 3, the PDF of I^1 can be obtained as follows*

$$f_{I_{C_3}^1}(x) = \int_0^x f_{I_m^1}(x-y)\, f_{I_s^1}(y) dy. \tag{25}$$

Corollary 2. *The probability of spatial miss detection can be approximated as*

$$P_{md} \approx \sum_{i=1}^{3} \int_0^\infty \widehat{P_{md}}(x)\, f_{I_{C_i}^1}(x) dx \mathbb{P}\{Case\ i\}, \tag{28}$$

where $\widehat{P_{md}}(x) = 1 - Q\left(\frac{\varepsilon - x - {\sigma_n}^2}{x + {\sigma_n}^2}\sqrt{N}\right)$, $f_{I_{C_i}^1}(x)$ is the approximated PDF of I^1 in case i, and $\mathbb{P}\{Case\ i\}$ is the probability of each case under $\mathcal{H}^1$.

IV. System-Level Performance Evaluation

In this section, we provide the coverage probability of D2D communications and the ASE of D2D networks.

A. Coverage Probability of A D2D User

Recall that a D2D-Tx can transmit with probability $P_d^0 = P_{fa}\beta_1 + (1-P_{fa})\beta_0$ under $\mathcal{H}^0$ and with probability $P_d^1 = (1-P_{md})\beta_1 + P_{md}\beta_0$ under $\mathcal{H}^1$, where P_{fa} and P_{md} are given in Corollary 1 and Corollary 2, respectively. Note that $\mathbb{P}\left(\Gamma > \varepsilon | \mathcal{H}^1, I^1\right) > \mathbb{P}\left(\Gamma > \varepsilon | \mathcal{H}^0, I^0\right)$ holds leading to $P_d^0 > P_d^1$. Statistically, all D2D-Txs will transmit with probability P_d^1, and the D2D-Txs that have no scheduled cellular users within the distance of $\mathcal{R}_s$ will transmit with probability $P_d^0 - P_d^1$. Therefore, the locations of active D2D-Txs are equivalent to a superposition of a PPP Φ_{d}^p with the density of $\lambda_d^p = P_d^1\lambda_d$ and a Poisson hole process (PHP) $\Phi_{\mathrm{d}}^h\left(\lambda_m, \mathcal{R}_s, \lambda_p, \mathcal{R}_s^{\mathrm{us}}, \lambda_d^h\right)$ where $\mathcal{R}_s^{\mathrm{us}} = 2\sigma_s + \mathcal{R}_s$ and $\lambda_d^h = \left(P_d^0 - P_d^1\right)\lambda_d$. We then give the coverage probability of a typical D2D user in the following Theorems and omit the detailed proof to save space.

Theorem 1. *When the typical D2D-Tx d_k is in Φ_d^p, the coverage probability of the D2D user is given in (26) at the bottom of the page, where* $\widehat{g}(a,b,s) = \int_{a-b}^{a+b} \arccos\left(\frac{t^2+a^2-b^2}{2ta}\right) \frac{2\lambda_d^h s P_d}{sP_d + t^\alpha} t dt$, $g(a,b,s) = \int_0^{b-a} \frac{2\pi\lambda_d^h s P_d}{sP_d+t^\alpha} t dt + \int_{b-a}^{b+a} \arccos\left(\frac{t^2+a^2-b^2}{2ta}\right) \frac{2\lambda_d^h s P_d}{sP_d+t^\alpha} t dt$ *when* $a \leqslant b$, $g(a,b,s) = \widehat{g}(a,b,s)$ *when* $a > b$, $l_k = \left\|d_k - u_k^d\right\|$, $f_{U_m}(r) = f_{B_m}(r)$, $f_c(r) = 2\pi\lambda_p r e^{-\pi\lambda_p r^2}$, $f_{U_{mh}}(r) = 2\pi\lambda_m r e^{-\pi\lambda_m\left(r^2 - {\mathcal{R}_s}^2\right)}$, $f_{ch}(r) = 2\pi\lambda_p r e^{-\pi\lambda_p\left(r^2 - (\mathcal{R}_s^{us})^2\right)}$.

Theorem 2. *When the typical D2D-Tx is in $\Phi_d^h\left(\lambda_m, \mathcal{R}_s, \lambda_p, \mathcal{R}_s^{us}, \lambda_d^h\right)$, the coverage probability of its attached D2D user is given in (27) at the bottom of the page, where $\widehat{g}(a,b,s)$ is given in Theorem 1.*

B. ASE of D2D Networks

The ASE of D2D networks can be obtained by considering the sets of Φ_{d}^p and $\Phi_{\mathrm{d}}^h\left(\lambda_m, \mathcal{R}_s, \lambda_p, \mathcal{R}_s^{\mathrm{us}}, \lambda_d^h\right)$ shown in the following theorem.

Theorem 3. *The ASE of D2D networks is given by*

$$ASE_D = \frac{T-\tau}{T}\left(\lambda_d^p \Theta \mathbb{P}^c_{u_k^{d,p}} + \lambda_d^h \mathbb{P}_{act}^{d,h} \Theta \mathbb{P}^c_{u_k^{d,h}}\right), \tag{29}$$

where $\Theta = \log_2\left(1+\gamma_d^{th}\right)$, $\mathbb{P}_{act}^{d,h} = \mathbb{P}\left\{\mathcal{H}^0\right\}$ given in (19), $\mathbb{P}^c_{u_k^{d,p}} = \mathbb{P}\left\{SINR\left(u_k^{d,p}\right) \geqslant \gamma_d^{th}\right\}$ in Theorem 1, and $\mathbb{P}^c_{u_k^{d,h}} = \mathbb{P}\left\{SINR\left(u_k^{d,h}\right) \geqslant \gamma_d^{th}\right\}$ in Theorem 2.

V. Simulation Results and Discussions

The simulated network operates at $P_0 = -30$ dBm, $\lambda_m = 5\times10^{-6}/\mathrm{m}^2$, $\lambda_p = 2\times10^{-5}/\mathrm{m}^2$, $\lambda_u = 1\times10^{-4}/\mathrm{m}^2$, $\lambda_d = 1\times10^{-4}/\mathrm{m}^2$, $n_b = 5$, $n_u = 15$, $\sigma_s = \sigma_u = 30$, $P_{fa}^* = 0.05$, $\alpha = 4$, $\eta = 0.5$, $\beta_0 = 0.8$, $\beta_1 = 0.16$, $N = 1$, ${\sigma_n}^2 = -110$ dBm, unless otherwise stated.

In Fig. 2, we compare the cumulative distribution function (CDF) of the received signal power at a typical D2D-Tx under the event $\mathcal{H}^1$. We can observe that the proposed analytical approximations can well approximate the Monte Carlo simulation results. The analytical approximations are efficient for computing the distributions of the received signal strength at a typical D2D-Tx. When the spatial spectrum sensing radius $\mathcal{R}_s$ increases, the average received signal strength at a D2D-Txs decreases under $\mathcal{H}^1$.

Fig. 3 shows the impact of the D2D-Tx spatial spectrum sensing radius $\mathcal{R}_s$ and the density of clustered small cells λ_p on the performance of spatial miss detection probability P_{md}. According to Neyman-Pearson criterion, the probability of spatial miss detection first increases and then decreases with respect to $\mathcal{R}_s$. This is because increasing $\mathcal{R}_s$ decreases the energy detection threshold ε, and when $\mathcal{R}_s$ approaches to the average distance between active uplink users, it becomes difficult to differentiate $\mathcal{H}^0$ and $\mathcal{H}^1$. In addition, we observe that, when small cells become denser, i.e., λ_p increases and/or n_b increases, P_{md} reduces since more active small cell users are around the SSS-based D2D-Tx and thus this increases the total received interference power at a D2D-Tx during SSS under the event $\mathcal{H}^0$. Moreover, the sensing radius that achieves maximum P_{md} decreases when λ_p increases.

In Fig. 4, we compare the ASE of D2D networks with respect to the D2D-Tx sensing radius $\mathcal{R}_s$ under different densities of small cell clusters λ_p and D2D-Txs λ_d. We can observe that the ASE of D2D networks decreases with increasing $\mathcal{R}_s$.

$$\mathbb{P}\left\{SINR\left(u_k^{d,p}\right) \geqslant \gamma_d^{th}\right\} \approx \exp\left\{-\frac{2\pi^2\left[\lambda_m \mathbb{E}\{P_{um}\}^{\frac{2}{\alpha}} + \left(\lambda_d^p + \lambda_d^h\right) P_d{}^{\frac{2}{\alpha}}\right]}{\alpha \sin\left(\frac{2\pi}{\alpha}\right)\left(\frac{\gamma_d^{th} {l_k}^\alpha}{P_d}\right)^{-\frac{2}{\alpha}}} - \frac{\gamma_d^{th} {l_k}^\alpha}{P_d}{\sigma_n}^2\right\} \int_0^\infty \frac{f_{U_m}(r)}{e^{-g\left(r, \mathcal{R}_s, \frac{\gamma_d^{th} {l_k}^\alpha}{P_d}\right)}} dr$$
$$\cdot \exp\left\{-2\pi\lambda_p \int_0^\infty x\left[1 - \exp\left(-n_b \int_0^\infty \frac{\frac{\gamma_d^{th} {l_k}^\alpha}{P_d}\mathbb{E}\{P_{us}\} r^{-\alpha}}{1 + \frac{\gamma_d^{th} {l_k}^\alpha}{P_d}\mathbb{E}\{P_{us}\} r^{-\alpha}} f_{U_s}(r|x) dr\right)\right] dx\right\} \int_0^\infty \frac{f_c(r)}{e^{-g\left(r, \mathcal{R}_s^{us}, \frac{\gamma_d^{th} {l_k}^\alpha}{P_d}\right)}} dr, \tag{26}$$

$$\mathbb{P}\left\{SINR\left(u_k^{d,h}\right) \geqslant \gamma_d^{th}\right\} \approx \int_{\mathcal{R}_s}^\infty \exp\left(\widehat{g}\left(r, \mathcal{R}_s, \frac{\gamma_d^{th} {l_k}^\alpha}{P_d}\right)\right) f_{U_m}(r) dr \int_{\mathcal{R}_s^{us}}^\infty \exp\left(\widehat{g}\left(r, \mathcal{R}_s^{us}, \frac{\gamma_d^{th} {l_k}^\alpha}{P_d}\right)\right) f_{ch}(r) dr$$
$$\cdot \exp\left\{-2\pi\lambda_p \int_0^\infty x\left[1 - \exp\left(-n_b \int_0^\infty \frac{\frac{\gamma_d^{th} {l_k}^\alpha}{P_d}\mathbb{E}\{P_{us}\} r^{-\alpha}}{1 + \frac{\gamma_d^{th} {l_k}^\alpha}{P_d}\mathbb{E}\{P_{us}\} r^{-\alpha}} f_{U_s}(r|x) dr\right)\right] dx - \frac{\gamma_d^{th} {l_k}^\alpha}{P_d}{\sigma_n}^2\right\} \tag{27}$$
$$\cdot \exp\left[-\frac{2\pi\lambda_m \mathbb{E}\{P_{um}\}}{(\alpha-2){\mathcal{R}_s}^{\alpha-2}} \frac{\gamma_d^{th} {l_k}^\alpha}{P_d} {}_2F_1\left(1, 1-\frac{2}{\alpha}; 2-\frac{2}{\alpha}; -\frac{\gamma_d^{th} {l_k}^\alpha \mathbb{E}\{P_{um}\}}{P_d {\mathcal{R}_s}^\alpha}\right) - \frac{2\pi^2\left(\lambda_d^p + \lambda_d^h\right)\left(\gamma_d^{th} {l_k}^\alpha\right)^{\frac{2}{\alpha}}}{\alpha \sin(2\pi/\alpha)}\right].$$

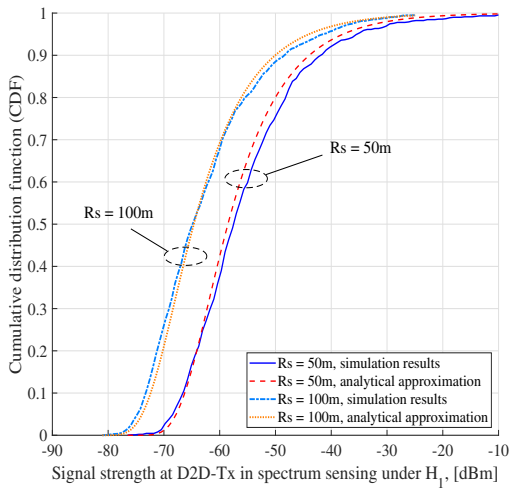

Fig 2: CDF of the received signal power at a typical D2D-Tx during spatial spectrum sensing under $\mathcal{H}^1$, where $\lambda_n = 3 \times 10^{-5}/\text{m}^2$.

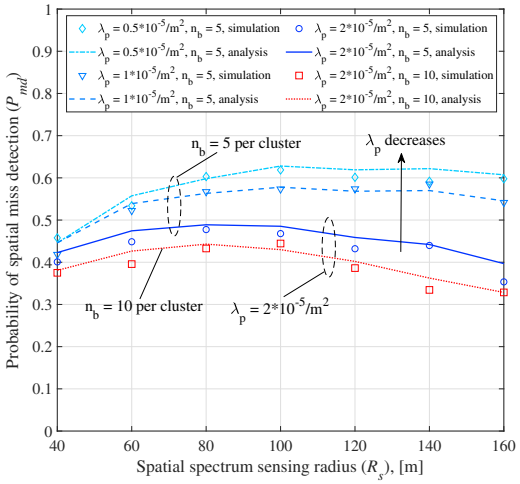

Fig 3: Probability of spatial miss detection P_{md} of a typical D2D-Tx regarding to the spatial spectrum sensing radius $\mathcal{R}_s$.

This is because when increasing $\mathcal{R}_s$, the average channel access probability of D2D-Txs decreases which reduces the number of active D2D pairs. Although the interference from D2D communications diminishes with $\mathcal{R}_s$, the ASE of D2D networks decreases since the number of active D2D pairs drops dominantly. When λ_p decreases, the ASE of D2D networks increases since the interference generated from cellular users decreases and the average channel access probability of D2D-Txs increases. When the interference from D2D to cellular networks is limited to a certain value, there exists a minimum spatial spectrum sensing radius and correspondingly a maximum ASE of D2D networks, which provides engineering design guidelines when implementing D2D communications in the two-tier clustered HetNets.

VI. Conclusions

In this paper, we model and analyze the SSS-based D2D communications in two-tier user-centric deployed HetNets. The average transmit power of uplink users, the probability of spatial false alarm and the probability of spatial miss detection of a typical D2D-Tx are characterized. In addition, we obtain the coverage probability and the ASE of D2D

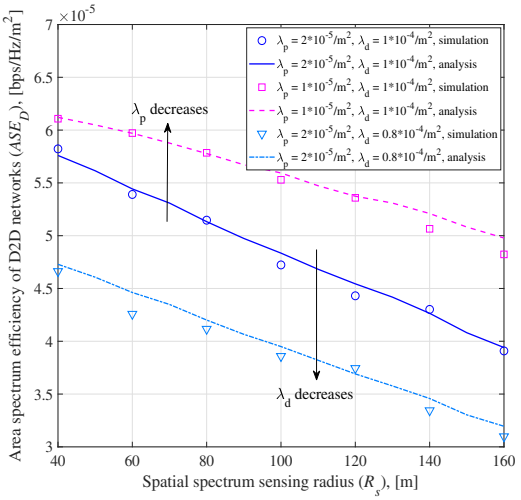

Fig 4: ASE of D2D networks with respect to the sensing radius $\mathcal{R}_s$.

networks. Finally, simulation results verify our theoretical analysis. In future work, it will be interesting to investigate the ASE of the entire network including both cellular and D2D communications under the constraint of cellular network's quality of service.

References

[1] R. I. Ansari, C. Chrysostomou, S. A. Hassan, M. Guizani, S. Mumtaz, J. Rodriguez, and J. J. P. C. Rodrigues, "5G D2D Networks: Techniques, Challenges, and Future Prospects," *IEEE Systems Journal*, vol. 12, no. 4, pp. 3970–3984, Dec 2018.

[2] B. Shang, L. Zhao, K. Chen, and X. Chu, "An Economic Aspect of Device-to-Device Assisted Offloading in Cellular Networks," *IEEE Transactions on Wireless Communications*, vol. 17, no. 4, pp. 2289–2304, April 2018.

[3] B. Shang, L. Zhao, K. Chen, and X. Chu, "Wireless-Powered Device-to-Device-Assisted Offloading in Cellular Networks," *IEEE Transactions on Green Communications and Networking*, vol. 2, no. 4, pp. 1012–1026, Dec 2018.

[4] B. Shang, L. Zhao, and K. Chen, "Enabling device-to-device communications in lte-unlicensed spectrum," in *2017 IEEE International Conference on Communications (ICC)*, May 2017, pp. 1–6.

[5] C. Saha, M. Afshang, and H. S. Dhillon, "3GPP-Inspired HetNet Model Using Poisson Cluster Process: Sum-Product Functionals and Downlink Coverage," *IEEE Transactions on Communications*, vol. 66, no. 5, pp. 2219–2234, May 2018.

[6] R. Atat, L. Liu, H. Chen, J. Wu, H. Li, and Y. Yi, "Enabling cyber-physical communication in 5g cellular networks: challenges, spatial spectrum sensing, and cyber-security," *IET Cyber-Physical Systems: Theory Applications*, vol. 2, no. 1, pp. 49–54, 2017.

[7] Z. Chen and M. Kountouris, "Decentralized Opportunistic Access for D2D Underlaid Cellular Networks," *IEEE Transactions on Communications*, vol. 66, no. 10, pp. 4842–4853, Oct 2018.

[8] H. Chen, L. Liu, T. Novlan, J. D. Matyjas, B. L. Ng, and J. Zhang, "Spatial spectrum sensing-based device-to-device cellular networks," *IEEE Transactions on Wireless Communications*, vol. 15, no. 11, pp. 7299–7313, Nov 2016.

[9] H. Chen, L. Liu, H. S. Dhillon, and Y. Yi, "QoS-Aware D2D Cellular Networks with Spatial Spectrum Sensing: A Stochastic Geometry View," *IEEE Transactions on Communications*, pp. 1–1, 2018.

[10] M. Haenggi, *Stochastic Geometry for Wireless Networks*. Cambridge University Press, 2012.

[11] W. Xiao, R. Ratasuk, A. Ghosh, R. Love, Y. Sun, and R. Nory, "Uplink Power Control, Interference Coordination and Resource Allocation for 3GPP E-UTRA," in *IEEE Vehicular Technology Conference*, Sep. 2006, pp. 1–5.

[12] S. M. Kay, *Fundamentals of Statistical Signal Processing: Detection Theory, vol. 2*. Englewood Cliffs, NJ, USA: Prentice-Hall, 1998.

[13] M. Haenggi, R. K. Ganti *et al.*, "Interference in large wireless networks," *Foundations and Trends in Networking*, vol. 3, no. 2, pp. 127–248, 2009.